Research Article

Pulmonary Circulation

Optimization of combined measures of airway physiology and cardiovascular hemodynamics in mice

Katrina W. Kopf[1,*], Julie W. Harral[2,*], Emily A. Staker[2], Megan E. Summers[2], Irina Petrache[2], Vitaly Kheyfets[3], David C. Irwin[4] and Susan M. Majka[2,5,6]

[1]Biological Resource Center, National Jewish Health, Denver, USA; [2]Department of Medicine, Division of Pulmonary, Critical Care & Sleep Medicine, National Jewish Health, Denver, USA; [3]Department of Bioengineering, Anschutz Medical Campus University of Colorado, Aurora, USA; [4]Department of Medicine, Division of Cardiology, Anschutz Medical Campus University of Colorado, Aurora, USA; [5]Department of Biomedical Research, National Jewish Health, Denver, USA; [6]Gates Center for Regenerative Medicine and Stem Cell Biology and Cardiology University of Colorado Medical Center, Aurora, USA

Abstract

Pulmonary hypertension may arise as a complication of chronic lung disease typically associated with tissue hypoxia, as well as infectious agents or injury eliciting a type 2 immune response. The onset of pulmonary hypertension in this setting (classified as Group 3) often complicates treatment and worsens prognosis of chronic lung disease. Chronic lung diseases such as chronic obstructive lung disease (COPD), emphysema, and interstitial lung fibrosis impair airflow and alter lung elastance in addition to affecting pulmonary vascular hemodynamics that may culminate in right ventricle dysfunction. To date, functional endpoints in murine models of chronic lung disease have typically been limited to separately measuring airway and lung parenchyma physiology. These approaches may be lengthy and require a large number of animals per experiment. Here, we provide a detailed protocol for combined assessment of airway physiology with cardiovascular hemodynamics in mice. Ultimately, a comprehensive overview of pulmonary function in murine models of injury and disease will facilitate the integration of studies of the airway and vascular biology necessary to understand underlying pathophysiology of Group 3 pulmonary hypertension.

Keywords

airway physiology, cardiovascular hemodynamics, Group 3 pulmonary hypertension, vascular remodeling

Date received: 30 November 2019; accepted: 11 February 2020

Pulmonary Circulation 2020; 10(1) 1–11
DOI: 10.1177/2045894020912937

Introduction

Group 3 pulmonary hypertension (PH) is classified as PH developing as a result of chronic lung diseases (CLDs).[1–3] CLDs are debilitating pathologies that impede overall tissue function, and as such, are a leading cause of mortality. Vasculopathy is a frequent comorbidity in CLD and may be characterized by deregulated or adaptive angiogenesis, remodeling, and loss of microvessels. Such remodeling may result in the development of PH, which significantly worsens prognosis and outcome.[4] PH is observed in many CLDs, including pulmonary fibrosis, chronic obstructive pulmonary disease (COPD)/emphysema, interstitial lung disease associated with systemic sclerosis as well as lymphangioleiomyomatosis.[1,5–13]

Although the underlying pathogenesis of vascular remodeling and dysfunction in COPD or fibrosis remains unclear, it is increasingly evident that they develop in the early stages of fibrosis,[8,10,14–25] as well as COPD.[26–31] More recently, type 2 immunity is thought to play a significant role in muscularization of the pulmonary vasculature.[32–36] Furthermore, despite advances in understanding some of the effects of pulmonary vascular remodeling to the development of emphysema, its effect on the phenotypic

*These authors contributed equally to this work.

Corresponding author:
Susan M. Majka, Division of Allergy, Pulmonary and Critical Care Medicine, 1400 Jackson St., K810, Denver, CO 80206, USA.
Email: susanmajka@mac.com

manifestations and severity of epithelial remodeling in CLD remain unknown. These gaps in knowledge underscore the need for future mechanistic investigations of the crosstalk between the vasculature and airways in CLD.

Typically, studies are performed separately to analyze either the cardiovascular hemodynamics or the airway physiology. Taken together, the literature supports that there is an inability to sustain functional tissue repair in both the vascular and epithelial compartments during disease. Therefore, we must begin to understand and model the underlying pathophysiology of pulmonary vascular deregulation, both alone and in combination with airway physiology in response to injury-induced disease.

These studies were designed to test the hypothesis that complementary airway physiology and cardiovascular hemodynamic analyses could be performed in tandem, on a single animal, to elucidate the interactions between the compartments necessary to maintain normal pulmonary tissue function and promote repair. Here, we provide a detailed protocol for the analysis of airway physiology with subsequent cardiovascular hemodynamics in a single mouse. Combining the use of these technologies increases the number of relevant endpoints that may be collected and potential numbers per group. These data collected in parallel will greatly enhance the understanding of two vital components of lung tissue, the vasculature and airways. These combined analyses will also enhance our understanding of the progression of vascular dysfunction in parallel to the development of CLD.

Methods

Study approval

The Institutional Animal Care and Use Committee at National Jewish Health approved all animal procedures and protocols. C57Bl6J mice were purchased from Jackson labs at 16 weeks of age and allowed to acclimate to Denver's altitude (~5280 ft) for 2.5 weeks. [Both 'flexivent' and 'flexiVent' are used. Please consider following consistency.]To validate the flexivent with hemodynamics measurements, mice were randomized into groups for a total of 7–9 animals per group. The groups included hemodynamics only (Hdx), flexivent only (Flexi), and flexivent + Hdx (Flexi + Hdx) (Table 1). For long-term studies, age matched mice were induced with low-dose tamoxifen (0.5 mg/18 g mouse) and housed for one year.[37] The groups included 10 wild type (WT 5 male and 5 female) and Wingless-related integration site (Wnt) activated mice (Bcatenin overexpression (BOE) 5 male (4 died) and 5 female, 1 died).

Surgical manipulation

Animals were induced with 4–5% isoflurane in room air at 1 L/min for approximately 2 min. The animal was then removed and placed in the supine position for passive ventilation via nosecone. The ventral neck and torso were shaved, and an incision was made down the midline of the neck, and tissue was blunt dissected to expose the trachea. A 1–2 mm incision was made in the trachea and a mouse endotracheal tube (Hallowell EMC, 201A3353) or 18 G metal cannula placed into the trachea with 4-0 suture. After intubation, the mouse was placed on 2–2.5% isoflurane ventilation via the flexiVent (SCIREQ, Montreal, QC, Canada). A pulse oximeter (Kent Scientific Physiosuite) was placed on a foot or thigh to obtain heart rate (HR) information. Relevant equipment is listed in Table 2.

Once the mouse was deeply anesthetized (as measured by failure of the toe pinch reflex and stable HR), 0.8–1.2 mg/kg of pancuronium was administered via intraperitoneal (i.p.) injection in order to prevent spontaneous respirations during the flexiVent analysis, which can interfere with data collection. Published studies indicated that pancuronium did not have significant effects on cardiovascular hemodynamics in porcine, rat, and humans with the exception of possible increases in HR.[38,39] Pancuronium has been used in concert with echocardiography to determine right ventricular structure in normal and hypoxic mice.[40] Alterations in HR may be used to monitor hemodynamic alterations due to anesthesia.[41]

Procedure 1: Airway physiology measurements

Respiratory function was measured using the flexiVent FX equipped with a module 2 (SCIREQ, Scientific Respiratory Equipment Inc., Montreal, Canada). The system artificially ventilated the animal with short (1–8 s) pressure–volume measurement maneuvers, called perturbations, and measured the resulting expiratory pressure and volume changes as a function of time against a physiological positive end expiratory pressure of 2.5–5 cmH_2O. Mathematical modeling was then applied to the signals generated from the perturbations resulting in the assessment of respiratory mechanics (flexiVent FX User Manual, SCIREQ). The following measures of respiratory mechanics were calculated from the flexiVent: inspiratory capacity (IC), total resistance (R), elastance (E), compliance (C), upper airway resistance, (Rus), respiratory system resistance (Rrs), Newtonian resistance (Rn), inertance (I), tissue damping (G), tissue elastance (H), and static compliance (Cst) (SCIREQ Method Note Understanding the flexiVent measures). The measures of most common interest in the literature include static compliance, a measure of the elastic properties of the respiratory system, and resistance of the respiratory system. Data were recorded continuously and analyzed offline. The airway physiology testing procedure took approximately 10 min per mouse, with the approximate surgery time of 5 min per animal.

Procedure 2: Cardiovascular hemodynamics – Non-survival surgery

Anesthesia was continued as one episode from the flexiVent analysis. At the conclusion of the airway physiology

Table 1. Pulmonary physiology measures per mouse.

Group	Sex	Weight (g)	HCT	RV/LV + S	RVSP (mmHg)	LVSP (mmHg)	CO (mL/min)	HR (beats/min)	Mean systemic pressure (mmHg)	PA pressure (mmHg)	Rrs ($cmH_2O.s/mL$)	Crs (mL/cmH_2O)	Ers (cmH_2O/mL)	Rn ($cmH_2O.s/mL$)	Cst (mL/cmH_2O)
Hdx	F	21.8	36	0.20	24.1	79.667	10.28	678	52.48	14.26					
Hdx	F	20.9	48	0.23	28.615	94.683	10.09	627		29.92					
Hdx	F	20.1	38	0.23	20.233	41.723	8.35	526	27.01	12.64					
Hdx	M	28.5		0.18	29.706	77.805	14.38	682	49.59	30.94					
Hdx	M	30.3	46	0.19	23.6	103.515	6.49	670	85.41	34.84					
Hdx	M	29.4	46	0.21	28.436	75.957	10.99	676	73.6	24.91					
Hdx	M	29	37	0.23	27.914	50.637	11.8	575	32.43						
Flexi	F	21.7		0.19				540[a]			0.421	0.0444	22.526	0.199	0.075
Flexi	F	20	49	0.21				576[a]			0.571	0.038	26.383	0.290	0.067
Flexi	F	21.1	53	0.18				525[a]			0.633	0.036	27.584	0.339	0.059
Flexi	M	31.8	46	0.17				579[a]			0.576	0.037	27.137	0.251	0.065
Flexi	M	30.2	48	0.22				450[a]			0.524	0.048	20.742	0.318	0.071
Flexi	M	28.7	40	0.20				350[a]			0.509	0.050	20.031	0.283	0.079
Flexi	F	18.9	46	0.18				550[a]			0.582	0.035	28.296	0.170	0.058
Flexi	F	17.6	42	0.24				525[a]			0.555	0.038	26.553	0.208	0.067
Flexi + Hdx	M	28.6	47	0.26	26.211	77.776	9.26	648	48.31	31.61	0.643	0.035	28.316	0.329	0.063
Flexi + Hdx	F	21.9	43	0.26	25.439	45.784	7.92	563	24.03	24.21	0.808	0.028	36.272	0.267	0.052
Flexi + Hdx	F	21.2	40	0.25	24.444	81.04	12.69	610	43.07	20.53	0.536	0.039	26.015	0.203	0.070
Flexi + Hdx	F	20.5	41	0.20	30.751	45.934	7.44	574	30.26		0.544	0.041	24.693	0.244	0.069
Flexi + Hdx	F	21.3	46	0.20	22.199	68.997	8.17	630	50.73	12.84	0.535	0.043	23.294	0.340	0.069
Flexi + Hdx	M	29	48	0.20	27.246	78.451	8.98	576	55.63	25.83	1.034	0.0524	19.105	0.293	0.079
Flexi + Hdx	M	30.3	45	0.22	24.47	108.113	9.67	638	73.68	17.2	0.436	0.048	20.877	0.216	0.073
Flexi + Hdx	M	27.7	44	0.21	28.647	76.463	10.8	632	58.98	29.68	0.392	0.055	18.255	0.213	0.087
Flexi + Hdx	M	31.7	43	0.24	20.285	38.573	10.71	598	27	19.31	0.472	0.046	21.603	0.253	0.076

[a]Monitored using a pulse oximeter.

Table 2. Major equipment.

RC2 rodent circuit controller	Vetequip Inc.	1452 N Vasco Rd. #303	Livermore, CA 94551	922100
TC-1000 temperature controller	CWE Inc.			08-13000
ADV500 advantage PV system	Transonic	34 Dutch Mill Road	Ithaca, NY 14850	
3.5 mm PV catheter				FTH-1212B-3518
4.0 mm PV catheter				FTH-1212B-4018
RA 834 data acquisition system	iWorx	62 Littleworth Road	Dover, NH 03820	IX-RA-834
Labscribe 4 software				
flexiVent	Scireq	6600 St-Urbain, Suite 300	Montreal, QC H2S 3G8 Canada	
Microvent 1	Hallowell EMC	239 West Street	Pittsfield, MA 01201	Discontinued

measurement, animals were immediately transferred to a Microvent 1 ventilator (Hallowell EMC, Pittsfield, MA) and isoflurane level maintained at 2.0–2.5% in 100% O_2 or 21% O_2/balance nitrogen for ventilated, open-chest studies. Peak breathing circuit pressure was maintained between 10 and 18 cmH_2O, breaths per minute at 50–150, and the oxygen flow at 0.3–0.5 lpm. A rectal temperature probe was placed (CWE, TC-1000), and body temperature maintained at 37 °C.

In an open-chest, solid-state catheterization procedure, ventricular function (right ventricle (RV) and left ventricle (LV)), pulmonary and systemic arterial pressures were

measured with a 1.2 French Pressure-Volume Catheter (FTH-1212B-3518 or 4018, Transonic Systems Inc., Ithaca, NY) inserted into the heart directly through the wall via a diaphragmatic approach. The procedure was developed as a modification of Pacher et al. describing hemodynamic measurement of LV hemodynamics.[42] Right and left ventricular functions were assessed by recording cardiac output (CO), maximal ventricular pressure (Pmax), afterload (Ea), end diastolic pressure volume relationship (EDPVR; a measure of stiffness/diastolic dysfunction), end systolic pressure volume relationship (Ees; a measure of contractility), and ventricular–arterial coupling (Ea/Ees).

A transverse incision was made across the width of the abdomen below the xiphoid process and the diaphragm cut away from the ventral chest wall to expose the heart and lungs. A length of 3-0 suture was placed underneath the inferior vena cava just anterior to the diaphragm to be used as a snare for occlusions. The pericardium was resected, and a small hole was made at the base of the RV with a 30-gauge needle. The pressure–volume catheter was then inserted in the hole and advanced along the length of the chamber. Bleeding is usually minimal due to the small size of the hole and the larger catheter plugging it.

At the conclusion of initial catheter placement, isoflurane was adjusted to 1.5–2% and the animal was allowed to equilibrate for approximately 2 min. The decrease in anesthesia was optimized to obtain hemodynamic measurements that are as close to normal physiology as possible without compromising the surgical depth of anesthesia. Anesthesia was checked to ensure that the animal was still in a surgical plane and the catheter was moved to obtain optimal positioning within the ventricle. Steady state hemodynamics were collected with short pauses in ventilation (up to 10 s) to eliminate ventilator artifact from the pressure–volume recordings. Occlusions of the inferior vena cava were also performed by pulling the abdominal snare taught (up to 10 s as well). This was to assess the end systolic pressure–volume relationship. The catheter was removed from the RV and another small incision was in the apex of the LV and the catheter placed along the length of the LV for measurement of steady state and occlusion data in the LV. The catheter may have also been advanced into the aortic arch for the collection of systemic pressure. One final incision was made in the RV, just below the pulmonary artery (PA) and the catheter was inserted to collect pulmonary arterial pressures. The order of data collection was optimized based on the priority of the information being collected, RV, LV, then PA. The order may be changed depending on a laboratory's specific hypothesis.

Data were recorded continuously and analyzed offline. Once the catheters were removed, the isoflurane level was set to 5%, the inferior vena cava was re-exposed, a 23-gauge needle inserted and the animal was exsanguinated. Direct heart puncture was used alternatively for animal exsanguination. Total time from induction to exsanguination was approximately 30 min.

Anesthetic regimen and monitoring

Isoflurane was chosen due to its minimal cardiosuppressant effects, ease of monitoring, and control.[42,43] The following anesthesia guidelines were implemented: (1) Animals were initially anesthetized with 4–5% isoflurane in room air at 1 L/min for approximately 2 min using a box. (2) All surgical manipulations were performed between 2 and 4% isoflurane in a surgical plane of anesthesia using a nose cone. (3) Following surgical manipulations, mice were maintained at 2.0–2.5% isoflurane for airway physiology and 1.5–2.0% isoflurane for hemodynamic measurements using a nose cone. (4) After the mice were either connected to the flexiVent or to the ventilator used for hemodynamic measurements, the paralytic pancuronium was administered IP (0.8–1.2 mg/kg). The paralytic was used as it is critical that there is no spontaneous respiratory effort during airway physiology measurements. Mice were maintained at a minimum of 2% isoflurane, as Tsukamoto et al.[44] found that 100% of mice were in a surgical plane of anesthesia at 2% isoflurane.

Anesthesia monitoring included HR monitoring as well as monitoring for an acute rise in HR rise upon toe pinch. With hemodynamic measurements, both blood pressure and HR were recorded and monitored continuously via direct catheterization of the heart. Our goal was to maintain the HR at the same levels observed during the flexiVent procedure, generally between 450 and 650 beats/min, and/ or as typically seen during hemodynamics at 2% isoflurane, with no response to toe pinch. In the instance that HR decreases below 300 beats/min, the isoflurane concentration may be reduced to 1.5% in order to prevent anesthetic death. However, during the course of this study, no mouse HR dropped below 300 beats/min.

Histology

Lungs were flushed with phosphate buffered saline (PBS) through the RV. A 20-gauge needle was connected to the plastic catheter and syringe adapter was connected to the endotracheal tube already in place. The chest cavity was completely dissected to expose the lung and heart field. Lungs were inflated under constant pressure using 1% low-melt agarose prepared in PBS heated to 42 °C. A manometer (Fisherbrand™ Traceable™ 06-664-18) kept in series to a 10 mL instillation syringe through a plastic tubing adapter (BD Intramedic™ 22-044083) was used to gauge infusion pressure. Two milliliters of warm agarose was added in the instillation syringe and lungs were slowly infused and a progressive and steady rise in the monometer to 25 cmH_2O was observed. The lung block was then dissected, placed on ice to solidify for 5–10 minutes, and fixed overnight in 16% formalin.

To prepare inflated lungs for histology and to ensure randomization of tissue sections, lungs were embedded in a 4% agarose mold. Once the agarose solidified, it was placed in a random orientation into a cutting box

(Exacto Machine & Tool, Indianapolis, IN). The lung was then cut on the transverse plane by sharp cryostat blades in 3 mm sections. The sections were placed into a histology cassette and processed for paraffin embedding. Tissue sections of 4 μm thick were cut. Standard H&E staining was performed.

Statistics

Data were analyzed by one-way ANOVA and T-test followed by Tukey's HSD post-hoc analysis. All analyses used JMP version 9.0.2. Data presented as ±standard error from the mean (±SEM). Significance was defined as p-value <0.05*, p-value <0.01**, or p-value <0.001***.

Results

Pressure–volume conductance catheter measurements of right ventricular systolic pressure (RVSP), left ventricular systolic pressure (LVSP), PA pressure, HR, and CO are commonly reported hemodynamic parameters for the study of vascular and cardiac dysfunction in murine models of chronic lung disease as well as pulmonary arterial hypertension. These endpoints are typically recorded using different mice. We sought to combine these analyses with measurements of airway physiology in order to present a comprehensive understanding of pulmonary tissue structure and function in a single animal, which may be applied to models of injury, disease, and tissue repair.

Age matched, 18.5-week-old male and female mice were randomized into three groups for comparison, Hdx, Flexi, or Flexi + Hdx. Mean body weight was significantly different between males and females; however, it was consistent throughout the groups (Fig. 1a, Table 2). Hematocrit and Fulton's index (RV/LV + S) was not significantly different between groups (Fig. 1b and c, Table 2). In humans, lung function can be measured using spirometry. However, this cannot be used in mice as it requires active participation from the subject or patient. Lung function was measured in the mouse using the flexiVent mouse ventilatory system. Measurement of airway physiology was performed alone or prior to the Hdx analysis. Values for typical endpoints were within the normal range and included total resistance (Rrs), system compliance (Crs), elastance (Ers), airway resistance (Rn), and static lung compliance (Cst) (Fig. 1d–h, Table 2).

Measurement of cardiovascular physiology was performed alone or following the flexiVent analysis, as one

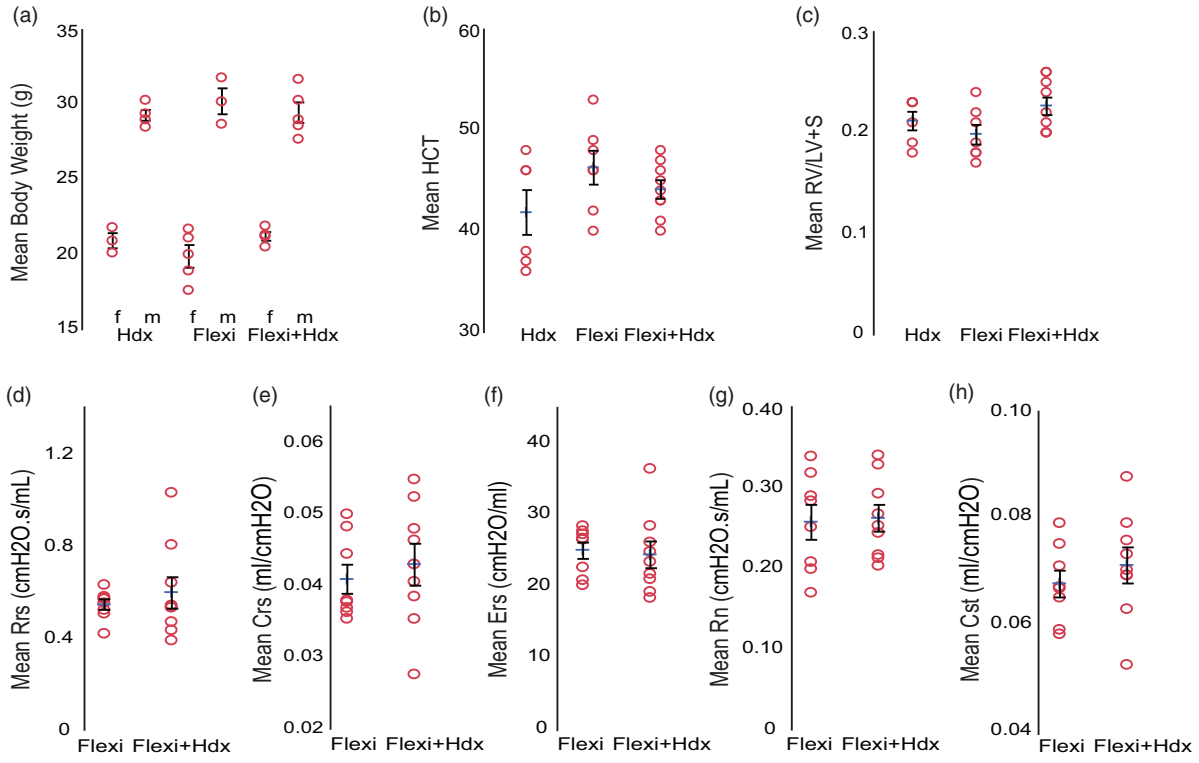

Fig. 1. Baseline comparisons between treatment groups. Measurements of lung and hemodynamic function in C57Bl6J mice (18.5 weeks old) that were anesthetized with inhaled isoflurane and i.p. pancuronium followed by measurement of hemodynamics only (Hdx), lung function only (Flexi), or the two combined (Flexi + Hdx). (a) Body weight, (b) hematocrit (HCT) and (c) RV/LV + S. flexiVent analysis of (d) total resistance (Rrs), (e) system compliance (Crs), (f) elastance (Ers), (g) airway resistance (Rn) and (h) static lung compliance (Cst). Data presented as mean (±SEM). The mean is indicated by +. n = 7–9 mice/group.

continuous event. Pressure–volume loops (P–V loops) were collected in the RV, followed by the LV and lastly the catheter was inserted into the PA, via the RV. The events may be reordered depending on the focus of the study. The RVSP is typically analyzed first when the major interest is remodeling of the pulmonary vasculature. A second penetration of the RV is necessary to reangle the catheter and reach the PA, thus either the LV or PA may follow. Values for typical endpoints fell within a normal range and did not differ between the Hdx compared to the Flexi + Hdx groups. Common endpoints included RVSP, LVSP, PA pressure, CO, HR, and systemic pressure (Fig. 2a–f, Table 2). P–V loops were also not significantly different between these two groups (Fig. 2g and h).

Since we implemented these methods on healthy WT mice, to validate their implementation in other rodent models, we performed flexivent + hemodynamic measurements on aged transgenic mice (~15 months of age). WT mice were compared to mice that had Wnt activated (BOE) specifically in mesenchymal vascular progenitor cells (MVPC).[37] We have previously described that MVPC specific Wnt activation results in lung microvascular dysfunction and remodeling. One year following tamoxifen induction, mice were analyzed. Body weight and hematocrit was lower in the BOE group relative to WT, while Fulton's index was similar (Fig. 3a–c). Measurement of airway physiology was performed combined with Hdx analysis (Table 3; Fig. 3d–h). Total airflow resistance (Rrs) in old WT mice was similar to young WT mice (Fig. 3d), whereas their elastance (Ers) was decreased (Fig. 3f). BOE group had significant changes compared to WT mice in both airflow resistance, which was increased (Fig. 3g), and in lung compliance (Crs), which was reduced, with corresponding increases in elastance (Fig. 3d and e). The systemic compliance (Cst) was also significantly decreased in

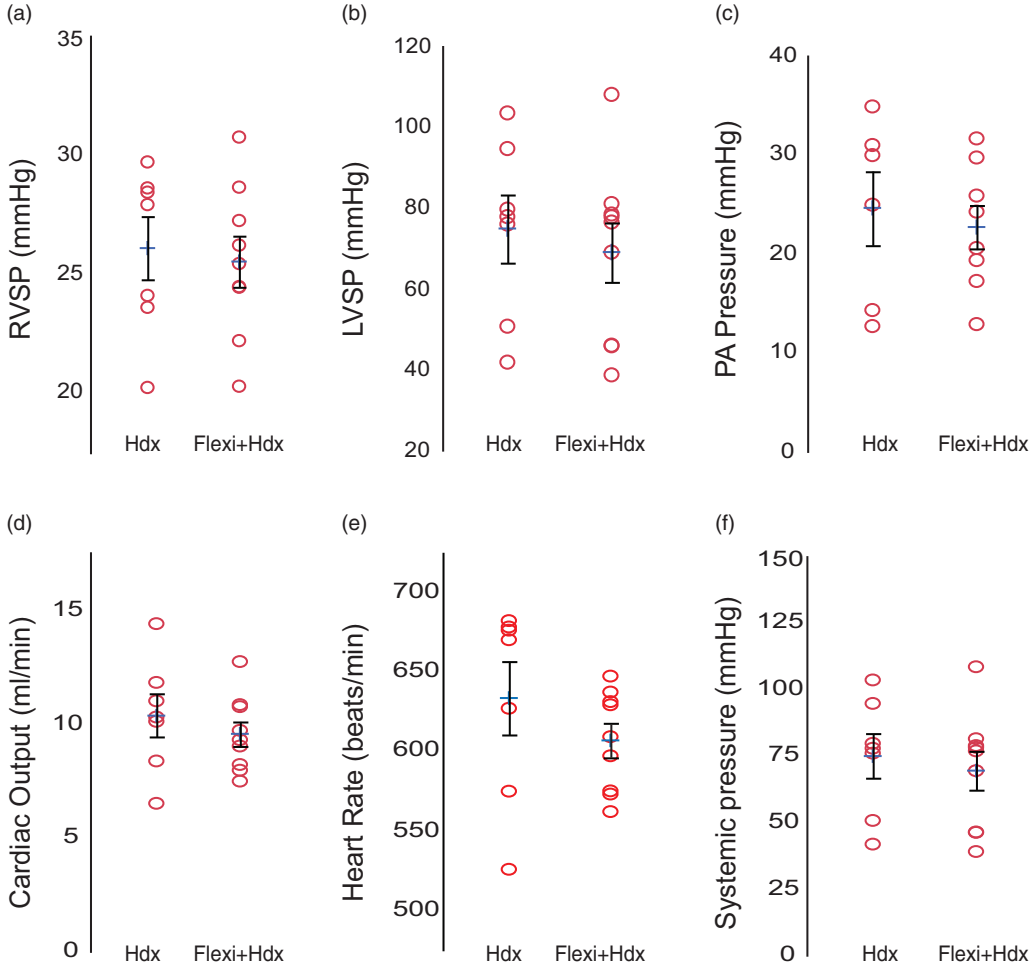

Fig. 2. Hemodynamic outcomes are not affected by flexiVent analysis. Hemodynamics (Hdx) measurement alone or following flexiVent analysis in C57Bl6J mice (18.5 weeks old) anesthetized with inhaled isoflurane and i.p. pancuronium. (a) A pressure transducer was placed in the right ventricle to measure RVSP or the (b) left ventricle to measure LVSP followed by (c) reinsertion into the RV and PA to measure PA pressure. (d) Cardiac output (CO), (e) heart rate, and (f) systemic pressure. The Hdx fell within a normal range and values were not significantly changed following flexivent analysis. Data presented as the mean (±SEM). The mean is indicated by +. n = 7–9 mice/group.

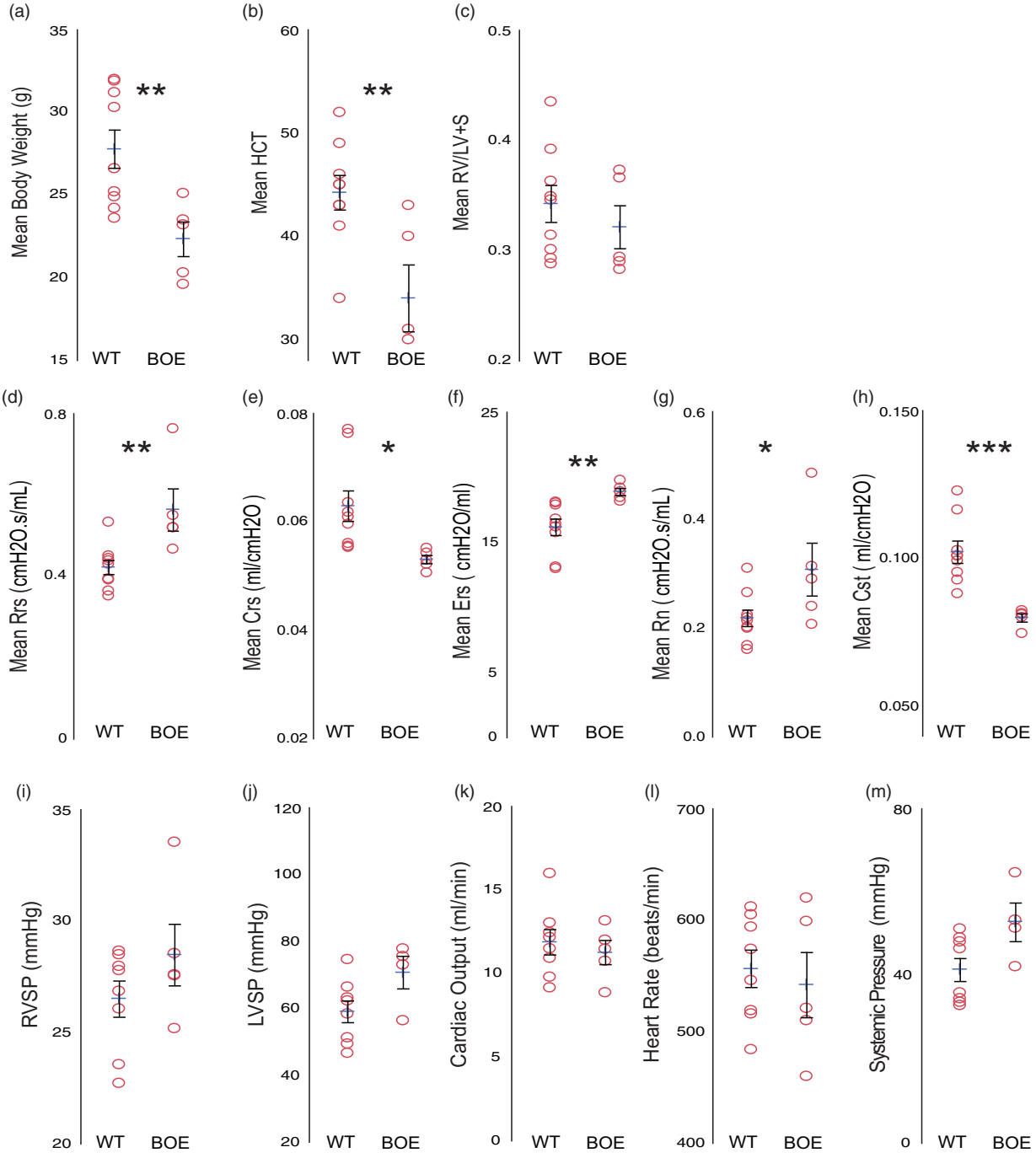

Fig. 3. Aged mice demonstrate increased lung stiffness in the absence of hypertension. flexiVent analsysis with hemodynamics (Hdx) measurement in WT or BOE mice one year following induction. (a) Body weight, (b) hematocrit (HCT)m and (c) RV/LV+S. flexiVent analysis of (d) total resistance (Rrs), (e) system compliance (Crs), (f) elastance (Ers), (g) airway resistance (Rn), and (h) static lung compliance (Cst). (i) A pressure transducer was placed in the right ventricle to measure RVSP or the (j) left ventricle to measure LVSP followed by reinsertion into the RV to measure (k) Cardiac output (CO), (l) heart rate, and (m) systemic pressure. Data presented as mean (±SEM). The mean is indicated by +. n = 5–10 mice/group.

the BOE lungs when compared to WT. Taken together these data suggest that aging increased lung stiffness and this effect was worse in the BOE group.

As with the young mice, measurement of cardiovascular physiology was performed following the flexiVent analysis. Values for typical endpoints fell within a normal range and did not differ significantly between the WT and BOE groups (Fig. 3i–m, Table 3). No indication of hypertension, pulmonary or systemic, was detected. The HR and CO of the WT aged mice fell within the range of the young mice

(between 550 and 650 beats/min; Figs. 3k and l and 2d and e), demonstrating there was no significant impact of pancuronium on cardiovascular hemodynamics.[41]

To determine the morphological aspects underlying the changes in lung function described above, as well as any impact of methodology in lung structure or inflammation, images of H&E stained lung sections were taken on a Nikon Eclipse 80i microscope using NIS Elements AR software (Fig. 4). As expected, there was no change in tissue morphology in groups that underwent hemodynamics or Flexi groups, when compared to the combination of Flexi + Hdx, regardless of age. Inflammation was only noted in BOE mice that had evidence of perivascular inflammation (Fig. 4a–f). There was no effect of measurement of both hemodynamics and flexivent on lung inflammation. Taken together these data illustrate that both airway and

Table 3. Pulmonary physiology measures per aged mouse.

Group	Sex	Weight (g)	HCT	RV/LV + S	RVSP (mmHg)	LVSP (mmHg)	CO (mL/min)	HR (beats/min)	Mean systemic pressure (mmHg)	PA pressure (mmHg)	Rrs (cmH_2O.s/mL)	Crs (mL/cmH_2O)	Ers (cmH_2O/mL)	Rn (cmH_2O.s/mL)	Cst (mL/cmH_2O)
WT	F	24.9	43	0.392	28.49	46.583	15.99	516	32.95	16.24	0.533	0.060	16.790	0.311	0.099
WT	F	24.2	49	0.301	23.56	74.623	12.16	605	35.97		0.451	0.056	18.027	0.214	0.093
WT	F	26.6	52	0.314	22.72	49.351	11.49	484	48.17	19.54	1.040	0.081	12.347	0.748	0.124
WT	F	25.2	45	0.346	26.06	62.25	9.15	612	51.27	13.99	0.438	0.062	16.196	0.266	0.101
WT	F	23.6	34	0.363							0.394	0.056	17.866	0.161	0.088
WT	M	30.3	46	0.293	26.85	58.341	9.79	546	34.57		0.430	0.061	16.433	0.225	0.103
WT	M	31.3	43	0.294	31.69	79.814	12.89	503	56.97	23.95	0.352	0.076	13.110	0.168	0.123
WT	M	31.2	45	0.349	27.97	66.384	10.92	574	46.54	23.62	0.444	0.055	18.093	0.202	0.101
WT	M	31.9	43	0.435	27.78	63.137	12.45	519	49.11	17.03	0.364	0.077	12.982	0.200	0.116
WT	M	32	41	0.288	28.65	51.208	13.03	594	33.72		0.391	0.064	15.746	0.220	0.095
BOE	M	23.2	40	0.294	27.59		10.74	510			0.520	0.052	19.173	0.241	0.080
BOE	F	19.6	30	0.366	28.542	77.796	12	521	64.71		0.519	0.055	18.155	0.291	0.082
BOE	F	20.3	43	0.29	25.177	73.002	8.86	599	51.46	13.16	0.467	0.053	18.888	0.207	0.081
BOE	F	23.5	31	0.373	27.547	56.337	13.16	620	42.24	14.87	0.550	0.054	18.444	0.315	0.081
BOE	F	25.1	26	0.283	33.537	75.529	11.46	460	53.38	16.24	0.763	0.051	19.768	0.486	0.075

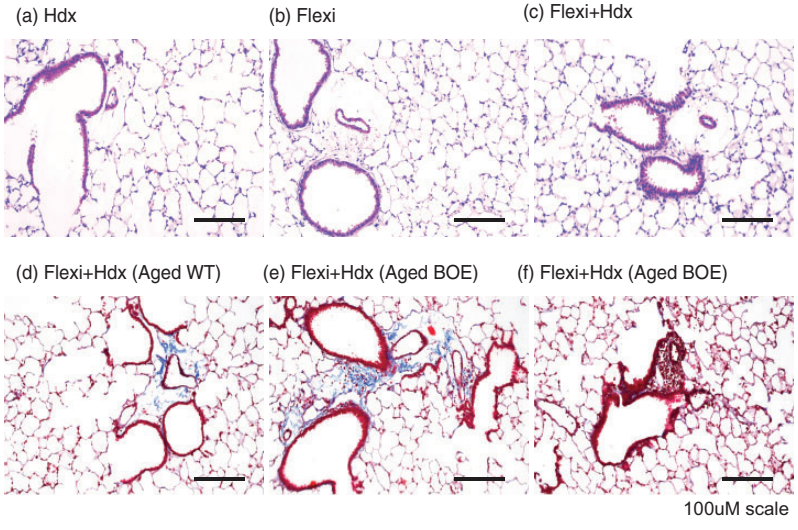

Fig. 4. Coupling flexivent and hemodynamics does not affect tissue morphology. Lungs were agarose inflated using constant pressure to obtain tissue for histological H&E or trichrome staining. Representative images were presented for young WT mice: (a) Hdx only, (b) flexiVent only, and (c) flexivent + Hdx or flexivent + Hdx for aged (d) WT and (e) and (f). BOE mice. Scale bars = 100 μM. n = 7–9 mice/group.

cardiovascular physiology measurements may be recorded sequentially using mouse models without any impact on tissue structure and inflammation.

Discussion

To provide a comprehensive overview of pulmonary function, we combined analyses of airway physiology with cardiovascular hemodynamics in mice. The integration of the airway and cardiovascular function is necessary to understand underlying pathophysiology that characterizes loss of tissue function. We found that the use of pancuronium as a neuromuscular blocking agent followed by continuous inhaled isoflourane, yielded reproducible airway function and cardiovascular hemodynamic results in naïve C57Bl6 mice. Taken together, these data documented that there was no significant difference between the Hdx group relative to group analyzed by both the flexiVent and Hdx procedures, in terms of physiology and histologic endpoints.

Because we did not find a difference in the respiratory or cardiovascular measures between the different groups, going forward, we have validated that it is possible to add pulmonary function testing with the flexiVent before hemodynamics. This increases the data that we can collect from each animal and reduces the number of animals required for answering our experimental questions, since we can perform both pulmonary and cardiac function tests on the same animal. It is also of great value to be able to have all of these data on a single animal so that cardiovascular function can be related to pulmonary function, since these two systems are so closely linked. Dayeh et al. found that mice with induced PH via pulmonary artery ligation had both an increased RVSP associated with the PH, as assessed with echocardiography and direct measures using a high fidelity catheter placed in the RV or LV, and also had an increased respiratory compliance, assessed with flexiVent.[45] These values were assessed in the same mice. By collecting data on pulmonary function testing and Hdx measurements in the same animals, we can help correlate these findings with human pathophysiology, furthering the ability to test treatments in experimental mouse models.

Prior to completing this experiment, we performed a brief pilot experiment to optimize anesthesia for combining flexiVent with Hdx. We tested ketamine (K) (80–120 mg/kg)/xylazine (X) (10–15 mg/kg)/pancuronium (P) (0.8–1.2 mg/kg). Although this combination (K/X/P) achieved adequate anesthesia, it caused greater depression in hemodynamic measurements compared to isoflurane and pancuronium. In addition, K/X/P was more difficult to titrate in a swift and precise manner. Mice anesthetized with either K/X/P or isoflurane with pancuronium had no difference between flexiVent and Hdx measurements in mice that had Flexi, Hdx, or flexiVent/Hdx combined. In addition, we were able to adequately anesthetize mice with isoflurane, an anesthetic with negligible impact on Hdx endpoints, which also offers the advantage of precise titration. Therefore, we determined that isoflurane with pancuronium was a superior anesthetic protocol for this experiment.

With regard to right ventricular function analysis, the measure of load-independent RV contractility is generally calculated as the slope of the end-systolic pressure–volume relationship (end-systolic elastance, Ees).[46] The gold standard methodology for measuring Ees in rodents is by creating multiple pressure–volume loops at varying loads by completing occlusions, a method we employed here.[47] The resulting Ees calculated from occlusion is found as the slope of a line fit to the end-systolic pressure points from multiple loops (known as ''multi-beat'' method). Often, investigators approximate this method by the single-beat method, which can estimate Ees from the pressure waveform of a single beat. However, the automated fitting procedure in single beat estimates can fail for certain pressure waveform morphologies[48] and suffers from repeatability issues because there is no agreed-upon methodology for identifying the true iso-volumic region in a pressure waveform.[49,50] Thus, in our study we evaluated cardiac contractility by the multi-beat method, which is the ''gold standard'' approach. Although occlusions are an invasive procedure, there was no difference between animals that had been analyzed by the flexivent first, further demonstrating that utilizing the flexivent does not disturb cardiac function.

This study has validated the ability to perform both pulmonary function testing and Hdx testing on in same animal, without impacting the findings for either testing modality. This combined procedure may be used to both decrease the required number of study participants as well as increase the data points collected from each participant. A fundamental question that remains is how deregulated angiogenesis may hinder the physiologic function of the lung. Establishing these mechanisms would provide key new insights into the pathogeneis of CLD and Group 3 PH and make it essential to examine the vascular and epithelial niches in murine models of emphysema and fibrosis. The ultimate goal of combining vascular and airway analyses into a single mouse is to identify a parallel time course of progression of injury to disease in both the cardiovascular and airway niches. Therefore, the next step is to validate this technology in well established murine models of chronic lung disease.

Acknowledgments

The authors would like to extend thanks to Dr Matthew Rosenbaum, DVM, MS, DACLAM, Director of the Biological Resource Center, National Jewish Health, for critical review of the manuscript. The authors would like to extend their thanks and greatest appreciation to Erica L Beatman for her expert technical assistance and training.

Authors' contributions

Conceptualization: JWH, KWK, DCI, SMM; Methodology: JWH, KWK, EAS, MES, DCI, SMM; Writing original draft: JWH, KWK, EAS, MES, DCI, SMM; Writing – review and

editing: JWH, KWK, EAS, MES, IP, DCI, SMM; Funding acquisition: IP, SMM; Resources: IP, SMM; Supervision: SMM.

Conflict of interest

The author(s) declare that there is no conflict of interest.

Funding

This work was funded by grants to SM Majka from NHLBI R01HL116597, NHLBI R01HL136449 and to I Petrache from R01HL077328.

References

1. Presberg KW and Dincer HE. Pathophysiology of pulmonary hypertension due to lung disease. *Curr Opin Pulm Med* 2003; 9: 131–138.
2. Pietra GG, Capron F, Stewart S, et al. Pathologic assessment of vasculopathies in pulmonary hypertension. *J Am Coll Cardiol* 2004; 43: 25S–32S.
3. Fishman A. Clinical classification of pulmonary hypertension. In: Rich S (ed.) *Clinics in chest medicine: pulmonary hypertension*. Philadelphia: W.B. Saunders Co., 2001, pp.385–391.
4. Austin ED, Kawut SM, Gladwin MT, et al. Pulmonary hypertension: NHLBI workshop on the primary prevention of chronic lung diseases. *Ann Am Thorac Soc* 2014; 11: S178–S185.
5. Barbera JA, Peinado VI and Santos S. Pulmonary hypertension in chronic obstructive pulmonary disease. *Eur Respir J* 2003; 21: 892–905.
6. Stevens D, Sharma K, Szidon P, et al. Severe pulmonary hypertension associated with COPD. *Ann Transplant* 2000; 5: 8–12.
7. Weitzenblum E and Chaouat A. Severe pulmonary hypertension in COPD: is it a distinct disease? *Chest* 2005; 127: 1480–1482.
8. Barratt S and Millar A. Vascular remodelling in the pathogenesis of idiopathic pulmonary fibrosis. *QJM* 2014; 107: 515–519.
9. Jankowich MD and Rounds SIS. Combined pulmonary fibrosis and emphysema syndrome: a review. *Chest* 2012; 141: 222–231.
10. Keane MP. Angiogenesis and pulmonary fibrosis. *Am J Respir Crit Care Med* 2004; 170: 207–209.
11. Antoniou KM, Margaritopoulos GA, Goh NS, et al. Combined pulmonary fibrosis and emphysema in scleroderma-related lung disease has a major confounding effect on lung physiology and screening for pulmonary hypertension. *Arthritis Rheumatol* 2016; 68: 1004–1012.
12. Condliffe R and Howard LS. Connective tissue disease-associated pulmonary arterial hypertension. *F1000Prime Rep* 2015; 7: 6.
13. Freitas CSG, Baldi BG, Jardim C, et al. Pulmonary hypertension in lymphangioleiomyomatosis: prevalence, severity and the role of carbon monoxide diffusion capacity as a screening method. *Orphanet J Rare Dis* 2017; 12: 74.
14. Distler JHW, Gay S and Distler O. Angiogenesis and vasculogenesis in systemic sclerosis. *Rheumatology* 2006; 45: iii26–iii27.
15. El-Chemaly S, Malide D, Zudaire E, et al. Abnormal lymphangiogenesis in idiopathic pulmonary fibrosis with insights into cellular and molecular mechanisms. *Proc Natl Acad Sci* 2009; 106: 3958–3963.
16. Hanumegowda C, Farkas L and Kolb M. Angiogenesis in pulmonary fibrosis: too much or not enough? *Chest* 2012; 142: 200–207.
17. Hirigoyen D, Burgos PI, Mezzano V, et al. Inhibition of angiogenesis by platelets in systemic sclerosis patients. *Arthritis Res Ther* 2015; 17: 332.
18. Hung C, Linn G, Chow Y-H, et al. Role of lung pericytes and resident fibroblasts in the pathogenesis of pulmonary fibrosis. *Am J Respir Crit Care Med* 2013; 188: 820–830.
19. Konttinen YT, Mackiewicz Z, Ruuttila P, et al. Vascular damage and lack of angiogenesis in systemic sclerosis skin. *Clin Rheumatol* 2003; 22: 196–202.
20. Manetti M, Guiducci S and Matucci-Cerinic M. The crowded crossroad to angiogenesis in systemic sclerosis: where is the key to the problem? *Arthritis Res Ther* 2016; 18: 36.
21. Strieter RM, Belperio JA and Keane MP. CXC chemokines in angiogenesis related to pulmonary fibrosis. *Chest* 2002; 122: 298S–301S.
22. Tzouvelekis A, Anevlavis S and Bouros D. Angiogenesis in interstitial lung diseases: a pathogenetic hallmark or a bystander? *Respir Res* 2006; 7: 82–82.
23. Yamashita M. Lymphangiogenesis and lesion heterogeneity in interstitial lung diseases. *Clin Med Insights Circ Respir Pulm Med* 2015; 9: 111–121.
24. Yamashita M, Iwama N, Date F, et al. Characterization of lymphangiogenesis in various stages of idiopathic diffuse alveolar damage. *Hum Pathol* 2009; 40: 542–551.
25. Farkas L and Kolb M. Pulmonary microcirculation in interstitial lung disease. *Proc Am Thorac Soc* 2011; 8: 516–521.
26. Sabit R, Bolton CE, Edwards PH, et al. Arterial stiffness and osteoporosis in chronic obstructive pulmonary disease. *Am J Respir Crit Care Med* 2007; 175: 1259–1265.
27. McAllister DA, Maclay JD, Mills NL, et al. Arterial stiffness is independently associated with emphysema severity in patients with chronic obstructive pulmonary disease. *Am J Respir Crit Care Med* 2007; 176: 1208–1214.
28. Alford SK, van Beek EJR, McLennan G, et al. Heterogeneity of pulmonary perfusion as a mechanistic image-based phenotype in emphysema susceptible smokers. *Proceedings of the National Academy of Sciences* 2010; 107: 7485–7490.
29. Yu N, Wei X, Li Y, et al. Computed tomography quantification of pulmonary vessels in chronic obstructive pulmonary disease as identified by 3D automated approach. *Medicine* 2016; 95: e5095.
30. Wiebe BM and Laursen H. Lung morphometry by unbiased methods in emphysema: bronchial and blood vessel volume, alveolar surface area and capillary length. *APMIS* 1998; 106: 651–656.
31. Barr RG, Mesia-Vela S, Austin JHM, et al. Impaired flow-mediated dilation is associated with low pulmonary function and emphysema in ex-smokers: the Emphysema and Cancer Action Project (EMCAP) study. *Am J Respir Crit Care Med* 2007; 176: 1200–1207.
32. Mickael CS and Graham BB. The role of type 2 inflammation in schistosoma-induced pulmonary hypertension. *Front Immunol* 2019; 10: 27–27.
33. Daley E, Emson C, Guignabert C, et al. Pulmonary arterial remodeling induced by a Th2 immune response. *J Exp Med* 2008; 205: 361–372.

34. Kumar R, Mickael C, Chabon J, et al. The causal role of IL-4 and IL-13 in *Schistosoma mansoni* pulmonary hypertension. *Am J Respir Crit Care Med* 2015; 192: 998–1008.
35. Rabinovitch M, Guignabert C, Humbert M, et al. Inflammation and immunity in the pathogenesis of pulmonary arterial hypertension. *Circ Res* 2014; 115: 165–175.
36. Chen G, Zuo S, Tang J, et al. Inhibition of CRTH2-mediated Th2 activation attenuates pulmonary hypertension in mice. *J Exp Med* 2018; 215: 2175–2195.
37. Gaskill CF, Carrier EJ, Kropski JA, et al. Disruption of lineage specification in adult pulmonary mesenchymal progenitor cells promotes microvascular dysfunction. *J Clin Investig* 2017; 127: 2262–2276.
38. Gursoy S, Bagcivan I, Durmus N, et al. Investigation of the cardiac effects of pancuronium, rocuronium, vecuronium, and mivacurium on the isolated rat atrium. *Curr Ther Res Clin Exp* 2011; 72: 195–203.
39. Grong K, Salminen P-R, Stangeland L, et al. Haemodynamic differences between pancuronium and vecuronium in an experimental pig model. *Vet Anaesth Analg* 2015; 42: 242–249.
40. Scherrer-Crosbie M, Steudel W, Hunziker Patrick R, et al. Determination of right ventricular structure and function in normoxic and hypoxic mice. *Circulation* 1998; 98: 1015–1021.
41. Estafanous FG, Brum JM, Ribeiro MP, et al. Analysis of heart rate variability to assess hemodynamic alterations following induction of anesthesia. *J Cardiothorac Vasc Anesth* 1992; 6: 651–657.
42. Pacher P, Nagayama T, Mukhopadhyay P, et al. Measurement of cardiac function using pressure-volume conductance catheter technique in mice and rats. *Nat Protoc* 2008; 3: 1422–1434.
43. Lindsey ML, Kassiri Z, Virag JAI, et al. Guidelines for measuring cardiac physiology in mice. *Am J Physiol Heart Circ Physiol* 2018; 314: H733–H752.
44. Tsukamoto A, Serizawa K, Sato R, et al. Vital signs monitoring during injectable and inhalant anesthesia in mice. *Exp Anim* 2015; 64: 57–64.
45. Dayeh NR, Tardif J-C, Shi Y, et al. Echocardiographic validation of pulmonary hypertension due to heart failure with reduced ejection fraction in mice. *Sci Rep* 2018; 8: 1363–1363.
46. Haddad F, Hunt SA, Rosenthal DN, et al. Right ventricular function in cardiovascular disease, part I: anatomy, physiology, aging, and functional assessment of the right ventricle. *Circulation* 2008; 117: 1436–1448.
47. Kass DA and Kelly RP. Ventriculo-arterial coupling: concepts, assumptions, and applications. *Ann Biomed Eng* 1992; 20: 41–62.
48. Brimioulle S, Wauthy P, Ewalenko P, et al. Single-beat estimation of right ventricular end-systolic pressure-volume relationship. *Am J Physiol Heart Circ Physiol* 2003; 284: H1625–H1630.
49. Philip JL and Chesler NC. Know your limitations: assumptions in the single-beat method for estimating right ventricular-pulmonary vascular coupling. *Am J Respir Crit Care Med* 2018; 198: 707–709.
50. Bellofiore A, Vanderpool R, Brewis MJ, et al. A novel single-beat approach to assess right ventricular systolic function. *J Appl Physiol (1985)* 2018; 124: 283–290.